







Research article

Studies of the *in vivo* bioresorption rate of composite filaments on the basis of polylactide filled with chitin nanofibrils or silver nanoparticles

Konstantin Vadimovich Malafeev^{1,2*}, Olga Andreevna Moskalyuk³,
Vladimir Evgenyevich Yudin^{1,2}, Dmitry Nikolayevich Suslov⁴, Elena Nikolaevna Popova²,
Elena Mikhaylovna Ivan'kova², Alena Alexandrovna Popova⁴

¹Peter the Great Saint Petersburg Polytechnic University, Saint Petersburg, Russia

²Institute of Macromolecular Compounds, Russian Academy of Sciences, Saint Petersburg, Russia

³Immanuel Kant Baltic Federal University, Kaliningrad, Russia

⁴Granov Russian Research Center for Radiology and Surgical Technologies, Saint Petersburg, Russia

Received 12 September 2023; accepted in revised form 24 November 2023

Abstract. The rates of *in vivo* bioresorption of composite monofilaments based on polylactide (PLA) containing chitin nanofibrils of two types (pure chitin (CN) or chitin modified with poly(ethylene glycol) (CN-PEG)) or silver nanoparticles stabilized with poly(*N*-vinylpyrrolidone) (Poviargol) were studied. The *in vivo* bioresorption rate and its dependence on the degree of orientational drawing of the samples (which varied from 1 in non-oriented samples to 4 in oriented samples) were investigated up to 12 months after implantation. Bioresorption of the samples was monitored using differential scanning calorimetry, scanning electron microscopy, and mechanical tests. Using the differential scanning calorimetry (DSC) method, it was shown that there is a gradual decrease in molecular weight due to a decrease in the temperatures of phase transitions and changes in peak shapes. It has also been shown that the addition of fillers containing water-soluble polymers accelerates the bioresorption of composite sutures. A thread made from pure PLA lost half its strength by the 9th month of implantation, whereas for threads with the addition of CN-PEG or Poviargol, this happened after 3.5 months. This causes leaching of water-soluble agents and changes in the supramolecular structure of the filament. This study shows the promise of using these composite threads as a suture material.

Keywords: polylactide, monofilament, biodegradation, chitin, silver nanoparticles, differential scanning calorimetry, scanning electron microscopy, strength, *in vivo* studies

1. Introduction

In recent decades, attention to using biomaterials for medical purposes has increased. This is because of their biocompatibility, biodegradability, and ease of processing. To date, many functional biopolymer composites have been developed to add value to raw biopolymers derived from natural sources or microbial systems [1]. Bioactive composites can be used in drug delivery systems [2], tissue engineering [3], cardiovascular [4], and thoracic surgery [5] and in many other areas of medicine [6].

An area of medical materials science, where the development of bioactive polymer composites has also begun, is the creation of suture materials. For hundreds of years, the primary function of suture material was to hold tissue edges together during wound healing. Gradually, the development of surgery has concluded that in addition to performing its main function, suture material can promote wound healing, resist surgical site infections (SSI), accelerate healing time, and simplify the patient's rehabilitation [7]. There are studies on the use of suture materials

*Corresponding author, e-mail: kostya_malafeev@mail.ru

© BME-PT

coated with stem cells, which increase the rate of wound healing after cardiac surgery [8]. Another part of the research on bioactive suture materials is devoted to imparting antibacterial properties. The authors [9] created an oriented nanofiber structure based on polylactide (PLA) and curcumin. The resulting threads had antibacterial and anti-inflammatory properties, promoted re-epithelialization, and accelerated wound healing. Other researchers achieve bioactivity by applying a bioactive coating to the thread surface. Blinov *et al.* [10] used a coating of silver nanoparticles to obtain suture threads with antibacterial activity. The resulting material did not cause a negative reaction in the tissues of the laboratory animals. In the article [11], the authors used a coating of PLA and polycaprolactone (PCL) to increase the bioresorption rate of a polydioxanone (PDO) thread. This made it possible to use these threads when suturing ligaments and tendons. As one can see, researchers are using different tactics to obtain the bioactivity of threads, from active coatings to creating nanostructured composite fibers.

In this study, we focused on creating PLA-based composite yarns with the addition of chitin nanofibrils (CN), chitin nanofibrils modified with polyethylene glycol (CN-PEG), and silver nanoparticles stabilized with polyvinylpyrrolidone (Poviargol). More details on the structure and mechanical properties of these fibers can be found in previous articles [12–14]. PLA suture material, due to its biocompatibility and biodegradability, can be absorbed by the body along with wound healing, so there is no need to remove sutures, which relieves patients from the pain associated with secondary suture removal [15]. Creating composites with the addition of natural polysaccharides such as chitin can improve the biocompatibility of synthetic fibers [1]. Chitin also has a wound-healing effect and can impart bioactivity to the composite suture [16]. The addition of silver nanoparticles can provide thread antibacterial activity with a prolonged effect [17].

The purpose of this study was to investigate the *in vivo* biodegradation of PLA-based composite fibers with the addition of chitin nanofibrils and silver nanoparticles. Assessment of the influence of the filler type and supramolecular structure of fibers on the rate of degradation and changes in their mechanical properties was carried out.

2. Materials and Methods

2.1. Materials

The following materials were used to prepare composite polymer-based filaments. Polylactide PLD9620, Purasorb, Purac (Amsterdam, The Netherlands) is a copolymer of L- and D-lactides (the monomer ratio is 96/4); its density is 1.29 g/cm³.

In the development of prototypes of surgical sutures with predicted bioresorption times, nanoparticles with various chemical structures and morphologies were used. Chitin nanofibrils (CN) were purchased from Mavi Sud s.r.l. (Aprilla, Italy). These nanofibrils have an anisotropic structure; their width is 20 nm, and their length varies from 600 to 800 nm. The structure of these particles has been studied using scanning electron microscopy and X-ray diffractometry [14, 18, 19].

To investigate the influence of the modification of chitin nanofibrils on the structure and properties of polylactide-based composite filaments, the surface of these nanofibrils was treated with poly(ethylene glycol). It has been demonstrated [14] that the modification of chitin nanofibrils with PEG contributes to better dispersion of chitin nanofibrils in the PLA matrix and enhances the mechanical strength of PLA filaments. In the subsequent text, the PEG-coated particles are denoted as CN-PEG. The modified nanoparticles were prepared using an aqueous suspension of chitin nanofibrils ($c = 2\%$, $\text{pH} = 1.9$). The suspension was neutralized until the pH reached 7 using 10% solution of sodium hydroxide (NaOH); then, a 2% solution of PEG was gradually added to the obtained mixture with constant stirring. The solvent was removed from the suspension by spray drying, and the final product consisted of light brown spherical particles with diameters ranging from 1 to 10 μm [14, 20]. Another filler used in the preparation of composite filaments was the silver-containing bactericidal agent Poviargol (Special Design and Technology Bureau ‘Tekhnolog’, Saint Petersburg, Russia) [13, 21]. Poviargol is a dark green powder that contains zero-valent silver metal in the form of nanoparticles 1–4 nm in diameter and a stabilizing agent (poly(*N*-vinylpyrrolidone)), which is the base for the plasma substituent Hemodez. The percentage of silver in these composites ranges from 7.5 to 8.5 wt%. The average size of the Poviargol powder particles varies from 2 to 16 μm [13].

2.2. Spinning of monofilaments

Before preparation, weighed amounts of polymers and fillers were dried in a vacuum oven (ULAB, Russia) at 80 °C for 4 h to remove residual moisture from the polymer and filler granules. Water may induce hydrolytic destruction of polylactide during high-temperature melt spinning, thereby deteriorating the mechanical strength and deformation characteristics of the final product [22].

Melt spinning of the monofilaments was performed using a DSM Xplore 5 ml microextruder (Sittard, The Netherlands). Polymer granules and a filler were loaded into the chamber heated to 220 °C and mixed with two screws for 5–10 min. It is necessary to delete the thermal history of the PLA, which this processing mode allows. After mixing, the melt was fed through a 1 mm-diameter die to the spool of the take-up unit. Immediately after leaving the die, the filament was cooled with a flat jet of compressed air; the diameter of the resulting non-oriented monofilament (here, the degree of drawing λ was taken as 1) varied from 350 to 400 μm (48–62 tex). To improve the stress–strain properties of the composite, the obtained monofilament was subjected to high-temperature 4-fold orientational drawing at 75 \pm 5 °C (in this case, the degree of drawing λ was taken as 4; the diameter of the oriented monofilament varied from 220 to 240 μm (19–22 tex)). The orientational drawing was conducted using hand-made special equipment (Figure 1).

2.3. *In vivo* investigation of the rates of bioresorption of the filaments

The experiments were conducted at the Granov Russian Research Center for Radiology and Surgical

Technologies. The study of *in vivo* resorption rates of the filaments involved 20 male Wistar rats (weight: 350–510 g) from the Rapolovo laboratory animal nursery. The animals were divided into four groups, each of which contained five animals. Pure PLA filaments were implanted into the animals of the first group; PLA+5 wt% CN filaments were implanted into the rats of the second group; PLA+5 wt% CN-PEG filaments were implanted into the rats of the third group; and the PLA+5 wt% Poviargol filaments were implanted into the rats of the fourth group. The surgeries were performed under anesthesia (Sol. Zoletil 50: 0.1 ml/0.1 kg animal body mass; Sol. Rometerum 20 mg/ml–0.0125 ml/0.1 kg animal body mass). The aponeurosis and parietal peritoneum were sutured with a continuous 4/0 Vicryl (Ethicon) suture (corresponding to 0.150–0.199 μm), and punctures were made 3 mm from the edge of the incision through the rectus muscles. The animal skin was replaced with a 4 mm interrupted suture with a 3/0 Lavsan thread (corresponding to 0.200–0.249 μm) manufactured by Lintex LLC (Saint Petersburg, Russia). For implantation of the filaments, laparotomy was performed along the white line of the abdomen. All experiments were performed under general anesthesia in accordance with the regulations concerning the use of laboratory animals (principles of European Convention (Strasbourg, 1986) and the Declaration of Helsinki developed by the World Medical Association concerning humane treatment of animals (1996)).

Bundles of non-oriented ($\lambda = 1$) filaments 30 mm in length were placed into the left part of the rat abdominal cavity, and samples with a degree of orientational drawing $\lambda = 4$ (40 mm in length) were implanted into the right part of the rat abdominal

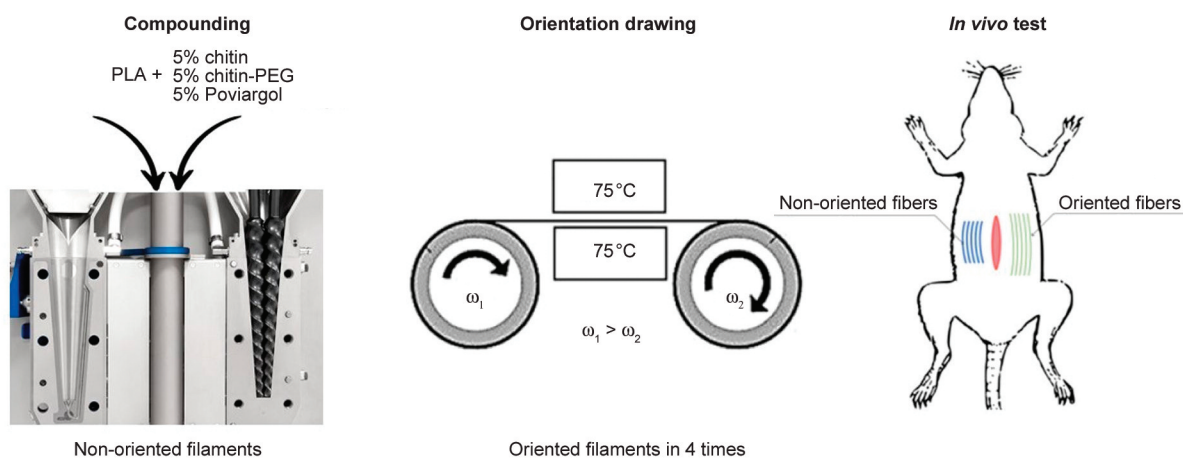


Figure 1. Scheme of sample preparation and fiber placement scheme during the *in vivo* test.

cavity, symmetrically to the incision line (Figure 1). Different lengths of filaments helped to distinguish the type of filament after degradation. The properties of the filaments were studied 1, 3, 6, 9, and 12 months after implantation; the animals were sacrificed, and the samples were removed. The degree of bioresorption of the implanted samples was estimated using several physical methods.

2.4. Mechanical tests

The mechanical properties of the composite-oriented filaments were studied by tensile tests using an Instron 5943 universal testing machine (Norwood, USA). The base length of the filaments was 30 mm, and the sample extension rate was 50 mm/min. The sample size of the mechanical tests was 5–7 samples. Stress–strain diagrams were used to determine the main characteristics of the filaments during stretching: tensile strength σ_b , the initial Young's modulus E_0 , and relative tensile strain ε_b .

2.5. Scanning electron microscopy

The structures of the composite filaments and fillers was studied by scanning electron microscopy (SEM) using a Carl Zeiss Supra-55 instrument (Jena, Germany). To visualize the distribution of filler particles inside the composite samples, the polymer filaments were fractured in liquid nitrogen, and the surfaces of the transverse fractures were studied. In addition, comparative studies of the filament surfaces were conducted. The samples were adhered to a special conductive sticky tape, covered with a thin platinum layer by spraying, and placed under a scanning electron microscope. Secondary electron images were obtained to reveal the topography of the samples. The accelerating voltage was 5 kV.

2.6. Differential scanning calorimetry

The investigations were conducted using a Netzsch DSC 204 F1Phoenix setup (Selb, Germany) in an inert medium (argon) in the temperature range of 80 to 280 °C. The heating rate was 10 °C/min. The degree of resorption of the samples was estimated on the basis of the phase transition temperatures and the corresponding enthalpy values.

3. Results and Discussion

3.1. Non-oriented filaments

The first step considers the mechanism of the resorption of non-oriented composite PLA filaments ($\lambda = 1$).

It was revealed that starting from the first month of implant exposure to the rat abdominal cavity, these filaments became fragmented or rolled up into dense coils, *i.e.*, their shape changed significantly. Therefore, it was not possible to perform mechanical tests on these samples. Structural changes occurring in the non-oriented filaments implanted in rats were estimated by DSC and SEM.

3.1.1. DSC studies

Non-oriented pure PLA filaments

Consider changes in phase transition temperatures that occur in the course of *in vivo* bioresorption of the non-filled PLA filaments. DSC curves of these samples are presented in Figure 2.

The shape of the DSC curve of the pure PLA filament (Figure 2) varies with filament implantation time. The mechanical and thermal histories of the samples are the same. For the sample implanted for less than 6 months, the glass transition temperature remained close to 66 °C when the exposure time increased up to 12 months; this parameter decreased slightly (down to 57 °C). A smooth decrease in the crystallization temperature of PLA (the maximum on the DSC exotherm) was observed during the entire period of implantation. At the beginning of the

Table 1. Thermal parameters of the non-oriented PLA filaments during the first heating scan.

Non-oriented	T_g [°C]	T_{cr} [°C]	T_m [°C]
PLA initial	63	124	151
PLA after 1 month <i>in vivo</i>	66	119	148
PLA after 6 months <i>in vivo</i>	65	106	147/154
PLA after 12 months <i>in vivo</i>	57	91	150

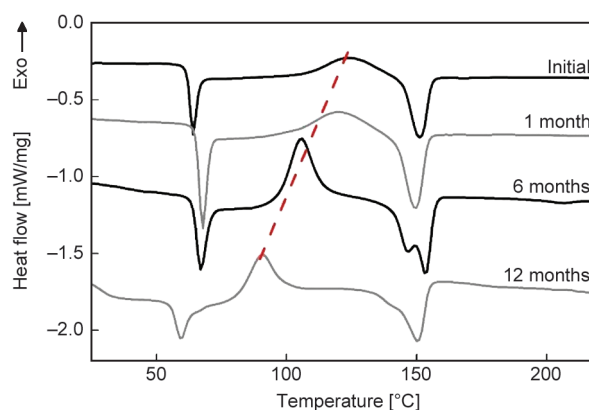


Figure 2. DSC curves of the non-oriented PLA filaments implanted into rats. The red dotted line shows the tendency toward a decrease in crystallization temperature.

experiment, the PLA crystallization temperature was equal to 120 °C, whereas in the final stage of the experiment (in 12 months), its value decreased to 90 °C. This effect can be explained by a reduction in the molecular mass of the polymer. PLA macromolecules become more mobile, which facilitates the crystallization of the polymer during heating in the DSC chamber. The melting temperature of a polymer depends on the crystallite size and the presence of defects [23]. A decrease in the number of defects and an increase in the crystallite size increase the melting temperature and vice versa. The change in the shape of the DSC melting peak is also related to changes in the molecular masses of the samples. When the PLA filament was implanted in rats for more than 6 months, the melting profile had two peaks, indicating the presence of two types of polymer chains with different molecular masses. When the sample remained in the living organism for 12 months, the melting peak broadened and a shoulder appeared near 140 °C. However, on the whole, the rate of PLA degradation is rather low, and the polymer retains its thermal parameters even after one year. The temperatures of the phase transitions are presented in Table 1. The obtained results suggest that hydrolytic destruction of PLA macromolecules (*i.e.*, reduction in its molecular mass) causes the appearance of imperfections in PLA crystallites, and their average sizes decrease during exposure of the filaments to a biologically active environment.

Non-oriented PLA+chitin nanofibrils filaments

The aim of the investigations of the bioresorption of PLA samples containing a natural filler (chitin nanofibrils) was to reveal the influence of the biological medium existing in the rat abdominal cavity on the rate of bioresorption of composite filaments. It has been reported earlier [24] that bioresorption can be accelerated in the presence of natural polymers at the expense of enzymatic hydrolysis. At the same time, bioresorption may slow down because the samples are placed into the abdominal cavity, which contains small amounts of liquid. The filament samples located relatively far from the center of the inflammation area are likely to be surrounded by the omentum, where bioresorption proceeds.

The composite samples were analyzed by differential scanning calorimetry. Figure 3 presents the DSC curves of the PLA-based filaments containing 5 wt% CN. It can be seen that with increasing implantation

time, the crystallization temperature of the sample decreases from 110 °C (1 month) to 95 °C (after 12 months). This result may indicate a decrease in the molecular mass of the polymer and, correspondingly, acceleration of the crystallization process [25–27]. The melting peak of this polymer splits into two peaks (143 and 152 °C), which indicates the formation of an inhomogeneous crystal structure of the polymer matrix (due to the appearance of smaller crystallites upon degradation of PLA macromolecules) (Table 2).

Degradation manifests itself more clearly in the DSC curves of the PLA samples filled with 5 wt% CN-PEG (Figure 4). The non-oriented PLA filament containing 5 wt% of PEG-modified CN has an amorphous structure, which is confirmed by the equal values of enthalpies of crystallization and melting (~24 J/g) determined by DSC scanning. The DSC curve includes a clearly seen ‘step’ that denotes the transition of the PLA matrix from the glassy state to the high-elasticity state ($T_g = 50$ °C). For the sample implanted for 6 months, the exothermic peak corresponding to crystallization is absent on the first DSC scan; therefore, it can be concluded that the ratio between the amounts of amorphous and crystalline phases in the filament changes. The endothermic peak (which corresponds to a melting process) is rather

Table 2. Thermal parameters of the non-oriented PLA+5 wt% CN filaments during the first heating scan.

Non-oriented	T_g [°C]	T_{cr} [°C]	T_m [°C]
PLA+5 wt% CN initial	63	110	150
PLA+5 wt% CN after 1 month <i>in vivo</i>	63	109	150
PLA+5 wt% CN after 6 months <i>in vivo</i>	60	102	144/153
PLA+5 wt% CN after 12 months <i>in vivo</i>	59	95	143/152

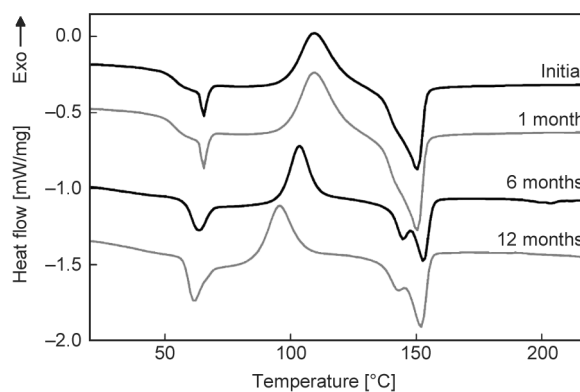
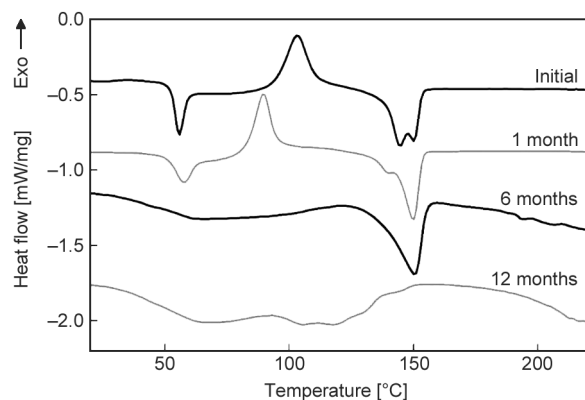


Figure 3. DSC curves of the non-oriented PLA+5 wt% CN samples removed from rat abdominal cavity after different periods of implantation.

Table 3. Thermal parameters of the non-oriented PLA+5 wt% CN-PEG filaments during the first heating scan.

Non-oriented	T_g [°C]	T_{cr} [°C]	T_m [°C]
PLA+5 wt% CN-PEG initial	54	103	145/150
PLA+5 wt% CN-PEG after 1 month <i>in vivo</i>	54	89	149
PLA+5 wt% CN-PEG after 6 months <i>in vivo</i>	–	–	150
PLA+5 wt% CN-PEG after 12 months <i>in vivo</i>	–	–	–

**Figure 4.** DSC curves of the non-oriented PLA+5 wt% CN-PEG samples removed from rat abdominal cavity after different periods of implantation.

smooth and has a minimum at approximately 150 °C. The temperatures of the phase transitions are presented in Table 3. The DSC curve obtained 12 months after implantation does not contain any clear exothermic or endothermic peaks, which may indicate a significant decrease in the molecular mass of the polymer.

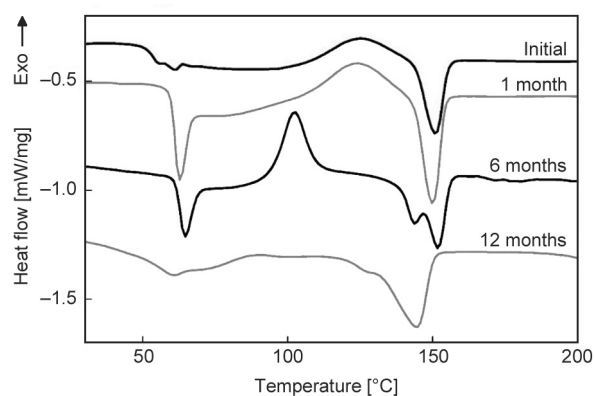
Non-oriented PLA+Poviargol filaments

Figure 5 presents the DSC curves of the non-oriented composite filaments based on PLA containing 5 wt% Poviargol.

The DSC thermogram (Figure 5) of the non-oriented filament studied 1 month after implantation contains an endothermic peak at approximately 120 °C, which indicates the amorphous structure of the initial filament and its crystallization during heating. The melting peak has a distinctive shape; the melting temperature is 150 °C. In the DSC curve obtained 6 months after the implantation of the sample, the exothermic peak corresponding to crystallization is shifted to 100 °C, which may indicate a reduction in the molecular mass of the polymer (Table 4). The melting peak broadens, and additional endo peaks appear; this result confirms the hypothesis of a decrease in

Table 4. Thermal parameters of the non-oriented PLA+5 wt% Poviargol filaments during the first heating scan.

Non-oriented	T_g [°C]	T_{cr} [°C]	T_m [°C]
PLA+5 wt% Poviargol initial	59	126	150
PLA+5 wt% Poviargol after 1 month <i>in vivo</i>	60	125	149
PLA+5 wt% Poviargol after 6 months <i>in vivo</i>	62	101	143/151
PLA+5 wt% Poviargol after 12 months <i>in vivo</i>	56	–	144

**Figure 5.** DSC curves of the non-oriented PLA+5 wt% Poviargol samples removed from rat abdominal cavity after different periods of implantation.

the average molecular mass and an increase in the polydispersity of the polymer sample. The DSC curve of the sample removed from a laboratory rat near the end of the experiment (in 12 months) does not contain the endothermic peak; thus, the ratio between the amounts of amorphous and crystalline domains in the sample changes during its presence in the rat organism.

3.1.2. Scanning electron microscopy

Non-oriented pure PLA filaments

Supramolecular structure of the samples was studied by scanning electron microscopy. Figure 6 presents the SEM images of the surfaces of the non-oriented PLA filaments after 12 months cleaved in liquid nitrogen. It can be seen in the micrograph of the sample implanted for 12 months that the fracture surface is nonuniform, and the heterogeneous elements have sizes of about 1 μm (Figure 6, yellow arrows). The result implies that degradation of the filaments proceeds according to the mechanism of homogeneous erosion (the uniform process over the whole sample). This indicates later stages of degradation when the liquid medium has already penetrated deep into the sample [28]. The possible reason for this is the

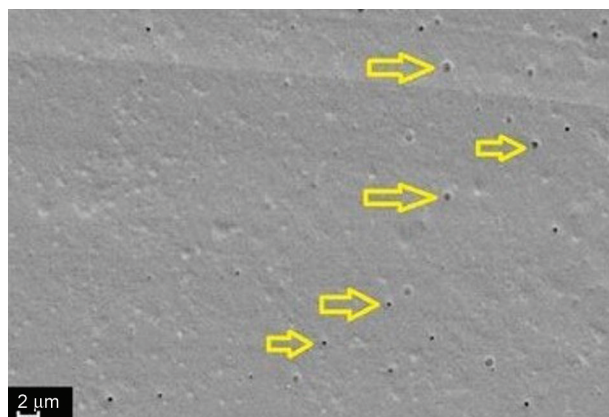


Figure 6. SEM micrograph of the pure PLA filaments implanted into rats for 12 months (cleaved surfaces obtained in liquid nitrogen).

amorphous structure of the filament. Diffusion of molecules of a liquid inside the sample with this structure proceeds more easily than that in the polymers containing crystalline domains [29].

Non-oriented PLA+ chitin nanofibrils filaments

Micrographs of fracture surfaces of the PLA-based filaments containing 5 wt% of CN (Figure 7) demonstrate that, 12 months after implantation, polylactide became relatively loose and numerous pores and cavities appeared, especially around the CN aggregates (Figure 7).

SEM micrographs of the cleaved surfaces of the filaments containing 5 wt% CN-PEG are shown in Figure 8. After 12 months, the entire filament is pierced with pores with sizes varying from 1 to 10 μm (which coincides with the size of filler particles). Thus, the presence of water-soluble PEG in the filler accelerates the degradation of non-oriented PLA

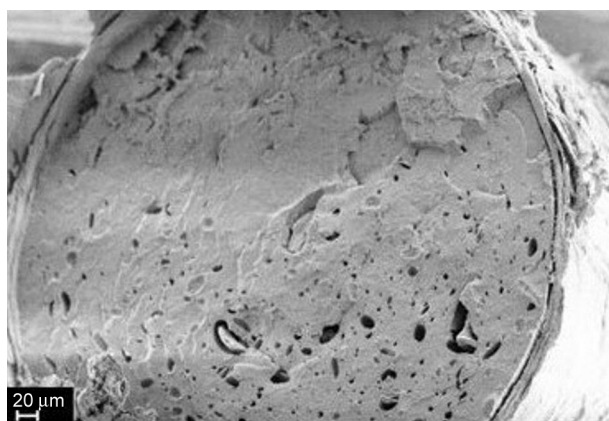


Figure 7. SEM micrograph of the non-oriented PLA+5 wt% CN filaments implanted *in vivo* for 12 months (cleaved surfaces obtained in liquid nitrogen).

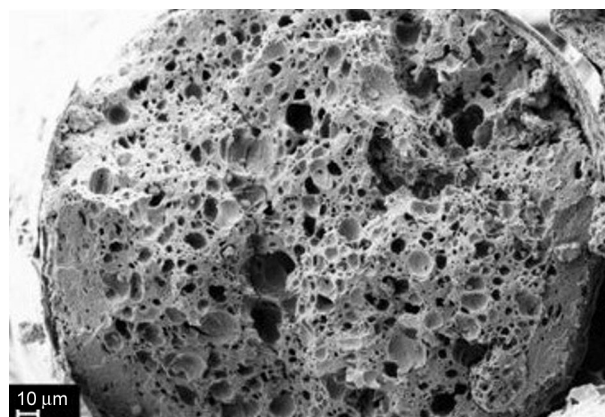


Figure 8. SEM micrograph of the non-oriented PLA+5 wt% CN-PEG filaments implanted *in vivo* for 12 months (cleaved surfaces obtained in liquid nitrogen).

filaments. This effect of accelerating degradation is also described in the article [30].

Non-oriented PLA+ Poviargol filaments

Figure 9 presents SEM images of PLA filaments filled with Poviargol (samples were cryo-cleaved in liquid nitrogen). It can be seen that 12 months after implantation, the cleaved surface is covered with numerous pores and cavities, whose sizes correspond to the dimensions of Poviargol granules (from 2 to 16 μm). This is because poly(*N*-vinylpyrrolidone), which is used as a stabilizer for nanoparticles, is a water-soluble polymer; during the *in vivo* experiments, body-liquids penetrate into the filament and dissolve PVP. Due to the appearance of pores, the surface area of a PLA filament becomes larger, and the bioresorption rate increases.

It has been demonstrated that the surface of fractured pure PLA filament has no visible signs of destruction;

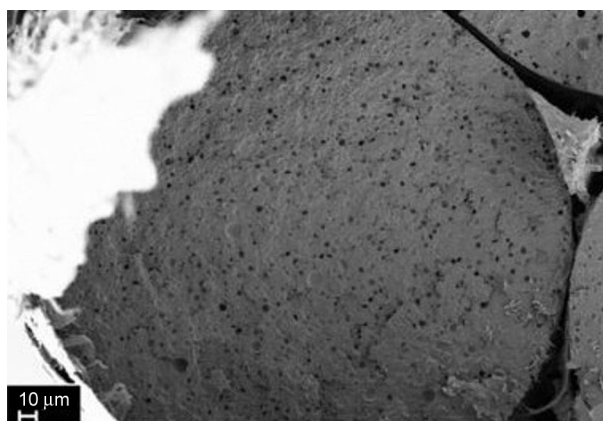


Figure 9. SEM micrograph of the non-oriented PLA-based composite filament containing 5 wt% of Poviargol taken 12 months after implantation (cleaved surfaces obtained in liquid nitrogen).

it is smooth and does not contain pores (Figure 6). When both types of chitin fillers or Poviargol are added, significant changes in the supramolecular structure of samples are revealed. The emerged pores and voids must contribute to the deterioration of the mechanical strength of these filaments (which is the most important characteristic for surgical sutures).

3.2. Filaments subjected to uniaxial drawing

3.2.1. Mechanical properties

In addition to DSC and SEM, mechanical tests were used to estimate the rate of resorption of the oriented filaments. Figure 10. shows the dependence of filament strength on implantation time. The zero value of mechanical strength indicates that the sample is too brittle for mechanical tests, although it can be removed from the body of a laboratory animal.

Because the studied filaments are intended for use as surgical sutures, the main parameter in bioresorption investigations was the time of the loss of 50% of the initial strength. Figure 10 demonstrates that the non-filled oriented PLA filaments lose half of their mechanical strength within 10 months following implantation, and after 12 months of implantation, they cannot bear the load. The addition of CN nanofibrils leads to acceleration of filament resorption; for example, the sample containing 5 wt% of CN loses half of its original strength in 6 months. The PLA filament containing 5 wt% CN-PEG loses 50% of its initial strength over the course of 3.5 months and disintegrates completely in 6 months. This fast degradation is most likely caused by the presence of water-soluble PEG in the filler; the dissolution of PEG leads to the appearance of pores inside the sample

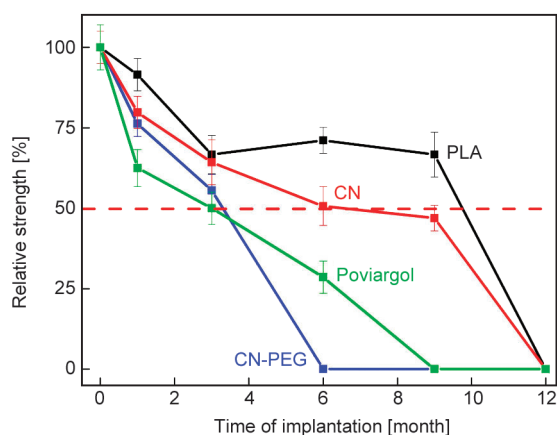


Figure 10. Dependences of the strength of pure PLA and composite filaments filled with various additives and subjected to 4-fold drawing on implantation time.

and, consequently, an increase in the area of contact between the sample and the environment. In addition, analysis of Figure 10 shows that the filaments containing 5 wt% of Poviargol subjected to 4-fold drawing lose 50% of their initial strength during the 3rd month of exposure, and the complete loss of mechanical strength occurs in the 9th month of the experiment. It is assumed that the accelerated resorption of these composite samples is caused by the structure of Poviargol, particularly the presence of water-soluble poly(*N*-vinylpyrrolidone) that covers the silver nanoparticles. Upon contact with an aqueous medium (buffer solution), PVP swells and dissolves, and a free volume appears inside the composite filament. This process facilitates the diffusion of biological liquids into the filament and increases the rate of PLA resorption. The optimal profile of bioresorption is the saving of mechanical strength in the first time of wound healing and subsequent fast resorption. The filaments with CN-PEG and Poviargol have a predictable time of 50% of the initial strength, which is approximately 3 months, which is similar to that of the commercial suture materials Monosyn and Monomax (B. Braun). Similar data were shown for the loss of half the mechanical strength in 12 weeks, as shown in the article [31]. The authors compared a polyhydroxybutyrate suture with commercial catgut and demonstrated less tissue response to the suture and a similar profile of changes in mechanical properties.

The experimental results demonstrated that the presence of fillers containing a water-soluble polymer accelerates the strength loss of PLA filaments due to changes in the supramolecular structure.

3.2.2. Differential scanning calorimetry

Oriented pure PLA filaments

Furthermore, we will consider changes in the PLA-based filaments subjected to 4-fold drawing that occur with time during the *in vivo* experiment. Figure 11 presents the DSC curves of the oriented filaments ($\lambda = 4$) removed from the rat body at different time periods. Note that the DSC curves of these samples implanted for less than 6 months contain either weakly pronounced exothermic peaks or minimums corresponding to polymer crystallization (Figure 11). When the DSC thermogram was obtained 12 months after implantation, no exothermic peaks were observed, which indicates changes in the supramolecular structure of the sample and in the ratio between

Table 5. Thermal parameters of the oriented PLA filaments (4-fold drawing) during the first heating scan.

Oriented (4-fold drawing)	T_g [°C]	T_{cr} [°C]	T_m [°C]
PLA initial	64	85	150
PLA after 1 month <i>in vivo</i>	67	93	148
PLA after 6 months <i>in vivo</i>	62	86	151
PLA after 12 months <i>in vivo</i>	67	–	148

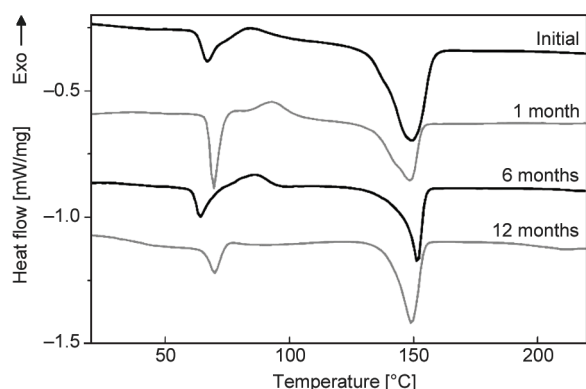


Figure 11. DSC curves of the pure PLA oriented filaments (4-fold drawing) implanted into rats for different periods.

the amounts of amorphous and crystalline fractions (Figure 11). The temperatures of the phase transitions are presented in Table 5.

Table 6. Thermal parameters of the oriented PLA+5 wt% CN filaments (4-fold drawing) during the first heating scan.

Oriented (4-fold drawing)	T_g [°C]	T_{cr} [°C]	T_m [°C]
PLA+5 wt% CN initial	68	–	147
PLA+5 wt% CN after 1 month <i>in vivo</i>	–	–	145
PLA+5 wt% CN after 6 months <i>in vivo</i>	68	–	150
PLA+5 wt% CN after 12 months <i>in vivo</i>	–	–	142

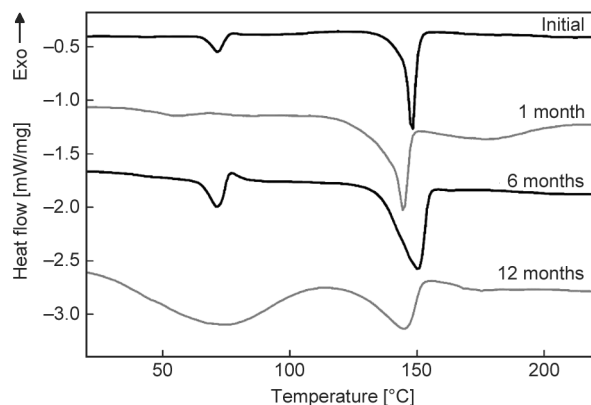


Figure 12. DSC curves of the oriented PLA+5 wt% CN filaments (4-fold drawing) obtained after different periods of implantation.

Oriented PLA+chitin nanofibrils filaments

As shown in Figure 12, the DSC curves of the samples containing 5 wt% CN exclude peaks corresponding to crystallization upon heating, which indicates the presence of crystalline domains in the oriented PLA filaments even under the conditions of the *in vivo* experiment. The melting peak of the initial sample has a clear shape and a distinct minimum at 145 °C. After 6 months of implantation, the filament remains crystalline, and the melting peak is located approximately at ~150 °C. After 12 months of the *in vivo* experiment, the melting peak at ~145 °C in the DSC curve of the sample containing 5 wt% CN changed shape and became broader; this was not observed for non-oriented filaments of similar composition.

The DSC patterns obtained for the oriented filaments with the addition of 5 wt% CN-PEG are different from those of the samples containing non-modified CN. The initial filament also has an amorphous-crystalline structure, and its melting temperature is about ~147 °C (Figure 13). After 6 months of implantation, when it was not possible to study the mechanical properties of the sample (Figure 13), the DSC thermogram showed that the crystalline structure and melting temperature (~147 °C) are retained.

Table 7. Thermal parameters of the oriented PLA+5 wt% CN-PEG filaments (4-fold drawing) during the first heating scan.

Oriented (4-fold drawing)	T_g [°C]	T_{cr} [°C]	T_m [°C]
PLA+5 wt% CN-PEG initial	–	–	147
PLA+5 wt% CN-PEG after 1 month <i>in vivo</i>	–	–	148
PLA+5 wt% CN-PEG after 6 months <i>in vivo</i>	–	–	145
PLA+5 wt% CN-PEG after 12 months <i>in vivo</i>	–	–	–

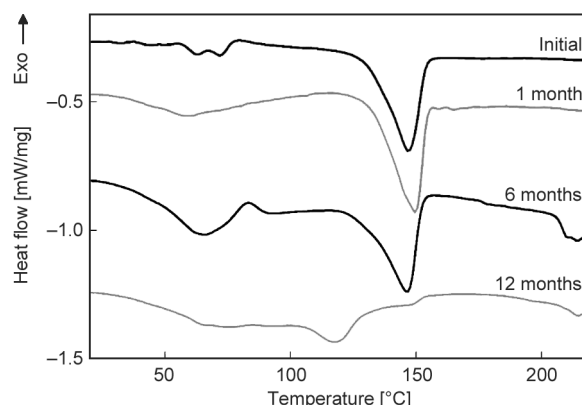


Figure 13. DSC curves of the oriented PLA+5 wt% CN-PEG filaments (4-fold drawing) obtained after different periods of implantation.

However, after 12 months of implantation, the melting peak broadens, and the minimum is located near 117°C, which is almost 40°C lower than that of the initial PLA. The temperatures of the phase transitions are presented in Table 6 and Table 7. The results indicate a significant degree of degradation of the composite material.

Oriented PLA+Poviargol filaments

Oriented PLA filaments containing 5 wt% Poviargol were also studied by DSC after implantation (Figure 14 and Table 8). Because there is no exothermic peak that corresponds to crystallization, it may be concluded that the filaments have a crystalline structure, which prevents the penetration of a liquid into the bulk of the polymer. All three first scan thermograms of the studied sample (obtained before the implantation, 6, and 12 months after implantation) show that the melting peaks are located at ~147°C, and $\Delta H_m = 27 \pm 2$ J/g. In other words, the rate of biodegradation of the PLA matrix is probably the same as that of the non-filled sample. The observed decrease in mechanical strength is not related to PLA biodegradation; rather, it is a result of the formation of pores inside the PLA filament.

Table 8. Thermal parameters of the oriented PLA+5 wt% Poviargol filaments (4-fold drawing) during the first heating scan.

Oriented (4-fold drawing)	T_g [°C]	T_{cr} [°C]	T_m [°C]
PLA+5 wt% Poviargol initial	70	–	147
PLA+5 wt% Poviargol after 1 month <i>in vivo</i>	67	–	147
PLA+5 wt% Poviargol after 6 months <i>in vivo</i>	62	–	148
PLA+5 wt% Poviargol after 12 months <i>in vivo</i>	–	–	147

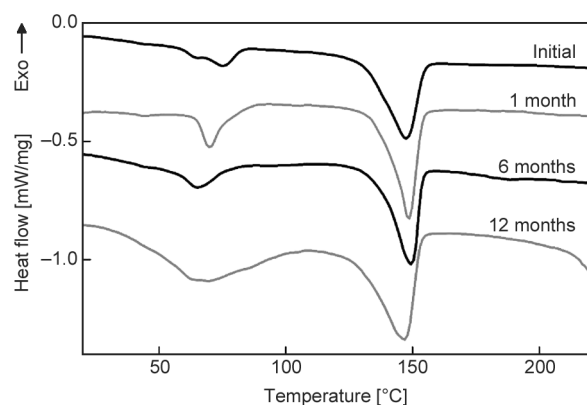


Figure 14. DSC curves of the oriented PLA+5 wt% Poviargol filament (4-fold drawing) at different stages of the *in vivo* experiment.

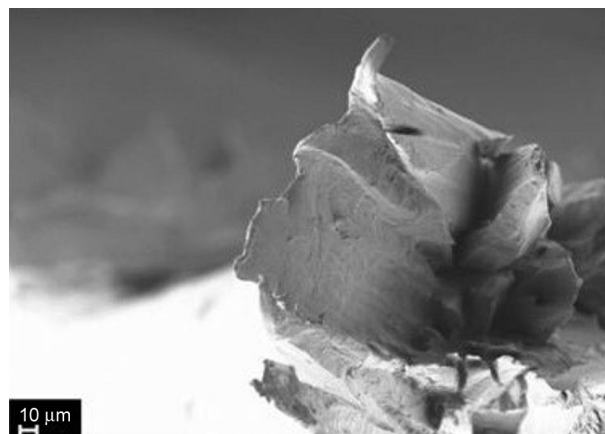


Figure 15. SEM micrograph of pure oriented PLA filaments taken after 12 months (cleaved surfaces obtained in liquid nitrogen).

3.2.3. Scanning electron microscopy

Oriented pure PLA filaments

Alterations in the supramolecular structure of the oriented PLA filaments were observed by microscopy. Figure 15 presents SEM images of the surfaces of PLA filaments cleaved in liquid nitrogen obtained 12 months after implantation.

The PLA filament implanted into the rat abdominal cavity for 3 months retained its rounded shape, although some defects 1 μm in size began to appear. Twelve months after the beginning of the experiment, it was not possible to obtain a smooth fracture surface because the filament collapsed.

Oriented PLA+chitin nanofibrils filaments

Figure 16a presents images of PLA filaments containing 5 wt% of CN taken 12 months after implantation. After 12 months of exposure, defects and cavities can be observed; it is obvious that degradation proceeded around the filler aggregates.

Figure 16b shows a comparison of the cleaved surfaces of the PLA filaments modified with 5 wt% CN-PEG. Analysis of the images of 4-fold drawn filaments demonstrates that the filament removed 12 months after the beginning of the experiment has many pores and voids with sizes up to 15 μm, which corresponds to the size of filler particles. It should be noted that it was not possible to prepare a sample with a smooth, cleaved surface after 12 months of exposure. Figure 16b shows cavities that indicate continuing bioresorption of the filament. The wound-healing effect of composite PLA filaments with CN will be considered in future studies.

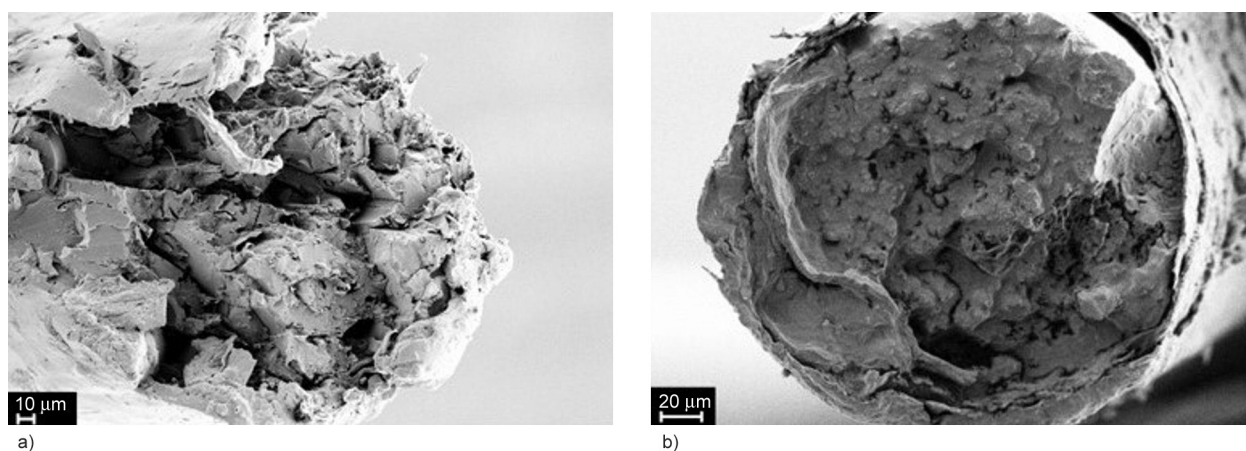


Figure 16. SEM micrographs of filled oriented filaments obtained at different stages of the *in vivo* experiment: a) PLA+5 wt% CN, 12 month; b) PLA+5 wt% CN-PEG, 12 months (cleaved surfaces obtained in liquid nitrogen).

Oriented PLA+Poviargol filaments

Investigation of the supramolecular structure of the filament containing 5 wt% of Poviargol (Figure 17) implanted into the rat abdominal cavity for 12 months revealed defects and an inhomogeneous structure of the sample. Considerable fragmentation and small pores are visible. This inhomogeneous structure mainly contributes to a decrease in the mechanical strength of the PLA filaments during the *in vivo* experiment. On the basis of previous data, it can be predicted that filaments containing Poviargol can have antibacterial effects delayed in time [12].

4. Conclusions

The rate of bioresorption of composite filaments on PLA containing 5 wt% of various fillers (chitin nanofibrils, chitin nanofibrils modified with poly(ethylene

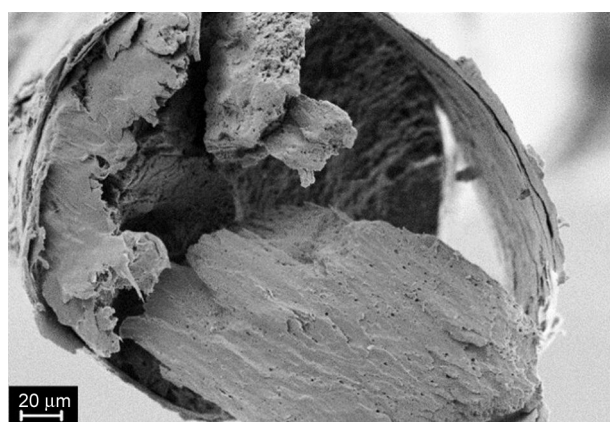


Figure 17. SEM micrograph of the oriented PLA+5 wt% Poviargol filament ($\lambda = 4$) removed 12 months after the beginning of the experiment (cleaved surface obtained in liquid nitrogen).

glycol), and Poviargol) was studied. The presence of these fillers in PLA accelerated the bioresorption of the monofilaments during the *in vivo* experiments. In the case of the composite monofilaments subjected to 4-fold orientational drawing and containing CN-PEG or Poviargol, the predictable period of loss of 50% of their mechanical strength was 3 times shorter than that for the non-oriented samples of the same composition (3.5 months of implantation). The addition of these fillers led to changes in the supramolecular structure of the filament during its stay in the living organism; SEM studies revealed the porous structure of the composite at the late stages of the experiment. In summary, it was shown that introducing fillers containing water-soluble polymers into PLA makes it possible to control the *in vivo* bioresorption rate of PLA filaments. Of the four groups studied, the threads with the addition of CN-PEG and Poviargol were the most interesting. With the help of these fillers, it was possible to effectively reduce the bioresorption period. Previously published articles have shown that the addition of these fillers increases the mechanical strength of PLA filaments [13]. In the next publications, it will be shown that these threads can meet the standards for surgical materials in terms of knot strength, and histological analyses and their mechanical properties in a liquid medium will also be investigated.

Acknowledgements

The work was financially supported by the Russian Science Foundation (grant 19-73-30003).

References

- [1] Park S.-B., Lih E., Park K.-S., Joung Y. K., Han D. K.: Biopolymer-based functional composites for medical applications. *Progress in Polymer Science*, **68**, 77–105 (2017).
<https://doi.org/10.1016/j.progpolymsci.2016.12.003>
- [2] Sharma S., Sudhakara P., Singh J., Ilyas R. A., Asyra M. R. M., Razman M. R.: Critical review of biodegradable and bioactive polymer composites for bone tissue engineering and drug delivery applications. *Polymers*, **13**, 2623–2688 (2021).
<https://doi.org/10.3390/polym13162623>
- [3] Tavoni M., Dapporto M., Tampieri A., Sprio S.: Bioactive calcium phosphate-based composites for bone regeneration. *Journal of Composites Science*, **5**, 227 (2021).
<https://doi.org/10.3390/jcs5090227>
- [4] Serruys P. W., Chevalier B., Dudek D., Cequier A., Carrié D., Iniguez A., Dominici M., van der Schaaf R. J., Haude M., Wasungu L., Veldhof S., Peng L., Staehr P., Grundeken M. J., Ishibashi Y., Garcia-Garcia H. M., Onuma Y.: A bioresorbable everolimus-eluting scaffold versus a metallic everolimus-eluting stent for ischaemic heart disease caused by de-novo native coronary artery lesions (ABSORB II): an interim 1 year analysis of clinical and procedural secondary outcomes from a randomised controlled trial. *The Lancet*, **385**, 43–54 (2015).
[https://doi.org/10.1016/s0140-6736\(14\)61455-0](https://doi.org/10.1016/s0140-6736(14)61455-0)
- [5] Lou W., Zhang H., Ma J., Zhang D., Liu C., Wang S., Deng Z., Xu H., Liu J.: *In vivo* evaluation of *in situ* polysaccharide based hydrogel for prevention of postoperative adhesion. *Carbohydrate Polymers*, **90**, 1024–1031 (2012).
<https://doi.org/10.1016/j.carbpol.2012.06.037>
- [6] Wang M.: Developing bioactive composite materials for tissue replacement. *Biomaterials*, **24**, 2133–2151 (2003).
[https://doi.org/10.1016/s0142-9612\(03\)00037-1](https://doi.org/10.1016/s0142-9612(03)00037-1)
- [7] Abhari R. E., Martins J. A., Morris H. L., Mouthuy P. A., Carr A.: Synthetic sutures: Clinical evaluation and future developments. *Journal of Biomaterials Applications*, **32**, 410–421 (2017).
<https://doi.org/10.1177/0885328217720641>
- [8] Guyette J. P., Fakharzadeh M., Burford E. J., Tao Z.-W., Pins G. D., Rolle M. W., Gaudette G. R.: A novel suture-based method for efficient transplantation of stem cells. *Journal of Biomedical Materials Research Part A*, **101**, 809–818 (2013).
<https://doi.org/10.1002/jbm.a.34386>
- [9] Richard A. S., Verma R. S.: Bioactive nano yarns as surgical sutures for wound healing. *Materials Science and Engineering: C*, **128**, 112334 (2021).
<https://doi.org/10.1016/j.msec.2021.112334>
- [10] Blinov A. V., Nagdalian A. A., Povetkin S. N., Gvozdenko A. A., Verevkinina M. N., Rzhepakovsky I. V., Lopteva M. S., Maglakelidze D. G., Kataeva T. S., Blinova A. A., Golik A. B., Osipchuk G. V., Shariati M. A.: Surface-oxidized polymer-stabilized silver nanoparticles as a covering component of suture materials. *Micromachines*, **13**, 1105 (2022).
<https://doi.org/10.3390/mi13071105>
- [11] Wu H., Guo T., Zhou F., Bu J., Yang S., Dai Z., Teng C., Ouyang H., Wei W.: Surface coating prolongs the degradation and maintains the mechanical strength of surgical suture *in vivo*. *Colloids and Surfaces B: Biointerfaces*, **209**, 112214 (2022).
<https://doi.org/10.1016/j.colsurfb.2021.112214>
- [12] Malafeev K., Moskalyuk O., Yudin V., Popova E., Ivankova E., Gordina E., Bozhkova S., Kanerva M.: Effects of silver nanoparticle on mechanical properties of polylactide composite yarns with different structure. *The Journal of the Textile Institute*, **113**, 2523–2530 (2021).
<https://doi.org/10.1080/00405000.2021.1995941>
- [13] Malafeev K. V., Moskalyuk O. A., Yudin V. E., Dobrovolskaya I. P., Popova E. N., Ivankova E. M., Kasatkin I. V., Morganti P., Kanerva M.: The influence of biodegradable dispersed fillers obtained by spray drying on the mechanical properties of polylactide fibers. *Nanotechnologies in Russia*, **15**, 456–465 (2020).
<https://doi.org/10.1134/s1995078020040084>
- [14] Malafeev K. V., Moskalyuk O. A., Yudin V. E., Morganti P., Ivankova E. M., Popova E. N., Elokhovskii V. Y., Vaganov G. V.: Study of physicochemical properties of composite fibers based on polylactide and modified chitin nanofibrils. *Polymer Science, Series A*, **62**, 249–259 (2020).
<https://doi.org/10.1134/s0965545x20030104>
- [15] Praharn C., Klinsukhon W., Padee S., Suwanamek N., Roungpaisan N., Srisawat N.: Hollow segmented-pie PLA/PBS and PLA/PP bicomponent fibers: An investigation on fiber properties and splittability. *Journal of Materials Science*, **51**, 10910–10916 (2016).
<https://doi.org/10.1007/s10853-016-0302-0>
- [16] Baharlouei P., Rahman A.: Chitin and chitosan: Prospective biomedical applications in drug delivery, Cancer treatment, and wound healing. *Marine Drugs*, **2022**, 460 (2022).
<https://doi.org/10.3390/md20070460>
- [17] Huq M. A., Ashrafudoulla M., Rahman M. M., Balusamy S. R., Akter S.: Green synthesis and potential antibacterial applications of bioactive silver nanoparticles: A review. *Polymers*, **14**, 742 (2022).
<https://doi.org/10.3390/polym14040742>
- [18] Yudin V. E., Dobrovolskaya I. P., Neelov I. M., Dresvyanina E. N., Popryadukhin P. V., Ivankova E. M., P.: Wet spinning of fibers made of chitosan and chitin nanofibrils. *Carbohydrate Polymers*, **108**, 176–182 (2014).
<https://doi.org/10.1016/j.carbpol.2014.02.090>

- [19] Dobrovolskaya I. P., Kasatkin I. A., Yudin V. E., Ivankova E. M., Elokhovskii V. Y.: Supramolecular structure of chitin nanofibrils. *Polymer Science Series A*, **57**, 52–57 (2015).
<https://doi.org/10.1134/s0965545x15010022>
- [20] Coltelli M. B., Cinelli P., Gigante V., Aliotta L., Morganti P., Panariello L., Lazzeri A.: Chitin nanofibrils in poly (Lactic acid) (PLA) nanocomposites: Dispersion and thermo-mechanical properties. *International Journal of Molecular Sciences*, **20**, 504 (2019).
<https://doi.org/10.3390/ijms20030504>
- [21] Kopeikin V. V., Panarin E. F., Santuryan Y. G., Afinogenov G. E., Pashnikova Z. A., Passage E. F., Budnikova T. I.: Water-soluble bactericidal composition and a method of its preparing. RU Patent 2088234C1, Russian Federation (1994).
- [22] Cairncross R. A., Becker J. G., Ramaswamy S., O’connor R.: Moisture sorption, transport, and hydrolytic degradation in polylactide. in ‘Twenty-seventh symposium on biotechnology for fuels and chemicals’ (eds.: McMillan J. D., Adney W. S., Mielenz J. R., Klasson K. T.) 774–785 (2006).
https://doi.org/10.1007/978-1-59745-268-7_63
- [23] Mandelkern L.: Crystallization of polymers: Volume 2, Kinetics and mechanisms. Cambridge University Press, New York (2004).
<https://doi.org/10.1017/CBO9780511535413>
- [24] Elsayy M. A., Kim K-H., Park J-W., Deep A.: Hydrolytic degradation of polylactic acid (PLA) and its composites. *Renewable and Sustainable Energy Reviews*, **79**, 1346–1352 (2017).
<https://doi.org/10.1016/j.rser.2017.05.143>
- [25] Santonja-Blasco L., Ribes-Greus A., Alamo R. G.: Comparative thermal, biological and photodegradation kinetics of polylactide and effect on crystallization rates. *Polymer Degradation and Stability*, **98**, 771–784 (2013).
<https://doi.org/10.1016/j.polymdegradstab.2012.12.012>
- [26] Godovsky Y. K., Slonimsky G. L., Garbar N. M.: Effect of molecular weight on the crystallization and morphology of poly(ethylene oxide) fractions. *Journal of Polymer Science Part C: Polymer Symposia*, **38**, 1–21 (1972).
<https://doi.org/10.1002/polc.5070380103>
- [27] Landel R. F., Nielsen L. E.: Mechanical properties of polymers and composites. CRC Press, Boca Raton (1993).
<https://doi.org/10.1201/b16929>
- [28] Oyama H. T., Kimura M., Nakamura Y., Ogawa R.: Environmentally safe bioadditive allows degradation of refractory poly(lactic acid) in seawater: Effect of poly (aspartic acid-co-L-lactide) on the hydrolytic degradation of PLLA at different salinity and pH conditions. *Polymer Degradation and Stability*, **178**, 109216 (2020).
<https://doi.org/10.1016/j.polymdegradstab.2020.109216>
- [29] Singh S., Patel M., Schwendemann D., Zacccone M., Geng S., Maspoch M. L., Oskman K.: Effect of chitin nanocrystals on crystallization and properties of poly(lactic acid)-based nanocomposites. *Polymers*, **12**, 726 (2020).
<https://doi.org/10.3390/polym12030726>
- [30] Rosli N. A., Karamanlioglu M., Kargarzadeh H., Ahmad I.: Comprehensive exploration of natural degradation of poly(lactic acid) blends in various degradation media: A review. *International Journal of Biological Macromolecules*, **187**, 732–741 (2021).
<https://doi.org/10.1016/j.ijbiomac.2021.07.196>
- [31] Chen X., Yang X., Pan J., Wang L., Xu K.: Degradation behaviors of bioabsorbable P3/4HB monofilament suture *in vitro* and *in vivo*. *Journal of Biomedical Materials Research Part B: Applied Biomaterials*, **92**, 447–455 (2010).
<https://doi.org/10.1002/jbm.b.31534>